Engineering Fracture Mechanics 134 (2015) 267–285

Contents lists available at ScienceDirect

Engineering Fracture Mechanics

journal homepage: www.elsevier.com/locate/engfracmech

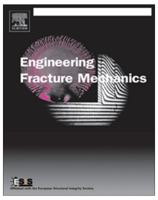

# Reverse identification of short–long crack threshold fatigue stress intensity factors from plain fretting crack arrest analysis

A. de Pannemaecker [a,b], S. Fouvry [a,*], J.Y. Buffiere [b]

[a] *Ecole Centrale de Lyon, LTDS, Ecully, France*
[b] *INSA de Lyon, MATEIS, Villeurbanne, France*

ARTICLE INFO

*Article history:*
Received 15 July 2014
Received in revised form 28 October 2014
Accepted 1 November 2014
Available online 27 November 2014

*Keywords:*
Fretting cracking
Crack arrest
Stress intensity factors
Crack propagation
Short crack behaviour

ABSTRACT

Plain fretting systematically implies crack arrest condition when the crack tip is far enough from the surface stressing. Considering such evolution, an original reverse FEM modelling of arrested cylinder/plane fretting cracks is introduced to extract the thresholds SIF of materials ($\Delta K_{th}$). Adjusting contact pressure and cylinder radius, short to long crack arrest responses are quantified and the corresponding "fretting" $\Delta K_{th}$ identified. Steel and aluminium alloy analyses (35NiCrMo16, AISI-1034, 7075-T6, 2024-T351) confirm the stability of this approach: the dispersion between long crack $\Delta K_{th}$ fretting estimations and conventional fatigue data is less than 10% whereas the short crack evolutions confirm the El-Haddad formalism.

## 1. Introduction

Fretting fatigue, consisting of a combination of contact fretting loading and bulk fatigue stress, is a critical issue in many industrial sectors [1–5]. Very severe fretting contact stress usually activates very fast crack nucleation, which can propagate until failure if the bulk fatigue stressing is sufficient. Such combined contact and fatigue stress causes drastic reduction in endurance, 4–5 times lower than the nominal fatigue limit [2]. Partial slip fretting load is characterised by very severe stress gradients with hot-spots at the trailing contact border when the friction coefficient is above 0.3. This local overloading causes fast crack nucleation and incipient 30–45° mixed-mode slant crack propagation. However, deeper below the surface, the mode I contribution increases, causing kinked bifurcation normal to the surface. This typical kinked crack propagation regime was formalised by Baietto et al. [6], applying Hourlier's criterion [7] which suggests that the crack path follows the direction which maximises the crack propagation rate. The evolution of the plain fretting Stress Intensity Factor (SIF) below the surface is non-monotonous (Fig. 1).

It displays an initial sharp increase followed by an asymptotic reduction below a critical depth, due to the very sharp decrease of contact stresses below the surface. SIF decreases until it reaches the material SIF threshold ($\Delta K_{th}$), inducing a crack arrest condition for a $b_{p,CA}$ "projected" crack arrest length, where $b_p$ is the projection of the real crack path along the normal direction (see A and C in Fig. 1). Although plain fretting leads systematically to a crack arrest condition, different patterns of evolution can be observed for fretting fatigue. Although the fretting SIF contribution systematically decreases with crack extension, the bulk fatigue contribution, in contrast, increases to the square root power of the crack length, leading to a typical "~" tilde-shaped SIF fretting fatigue evolution. For small fatigue stress, the SIF value crosses the material

---

* Corresponding author.
*E-mail address:* siegfried.fouvry@ec-lyon.fr (S. Fouvry).

http://dx.doi.org/10.1016/j.engfracmech.2014.11.001
0013-7944/© 2014 Elsevier Ltd. All rights reserved.

## Nomenclature

| | |
|---|---|
| $a$ | half width of the contact area |
| $b$ | crack length |
| $b_e$ | rapidity index of stabilisation |
| $b_0$ | short crack/long crack transition |
| $b_p$ | maximum projected crack length (to the normal of the surface) |
| $b_{p,CA}$ | maximum projected crack length related to the crack arrest condition |
| $b_{p,CA(n)}$ | normalised $b_{p,CA}$ versus the contact radius |
| $z$ | subsurface axis |
| $C$ | hardening coefficient |
| $c$ | radius of the stick zone |
| $E$ | Young's modulus |
| $H_{q_{max}}$ | slope of the curve $b_{p,CA}$ ($q_{max}$) |
| $K_{Imax}$ | maximum mode I stress intensity factor (at the trailing contact border when $+Q^*$) |
| $K_{Imin}$ | minimum mode I stress intensity factor (at the trailing contact border when $-Q^*$) |
| $L_i$ | length of the crack segment $i$ |
| $N$ | total number of fretting cycles |
| $P$ | linear normal force |
| $Q$ | fretting linear tangential force |
| $Q^*$ | fretting linear tangential force amplitude |
| $Q_\infty$ | asymptotic value corresponding to the stabilised cyclic regime |
| $q(x)$ | surface shear profile |
| $q_{max}$ | maximum surface shear |
| $q_{max,CN}$ | maximum surface shear inducing crack nucleation |
| $R$ | radius of the cylinder pad |
| $R_K$ | SIF ratio at the crack tip ($K_{Imin}/K_{Imax}$) |
| $R_\sigma$ | fatigue stress ratio ($\sigma_{min}/\sigma_{max}$) |
| $R_{Q^*}$ | fretting stress ratio ($Q^*_{min}/Q^*_{max}$) |
| $R_0$ | flow stress of the non-hardening material |
| $W$ | thickness of the plane specimen |
| (K–T) | related to the Kitagawa–Takahashi formalism |
| (E-H) | related to the El-Haddad formalism |
| (P-L) | related to the Power Law formalism |
| 35NCD15 | related to 35NiCrMo16 steel alloy |

*Greek letters*

| | |
|---|---|
| $\Delta K$ | nominal Stress Intensity Factor Range |
| $\Delta K_0$ | nominal threshold stress intensity factor range value related to the long crack arrest condition (constant value) |
| $\Delta K_{0(fr)}$ | range of the fretting long crack arrest stress intensity factor threshold |
| $\Delta K_{th}$ | crack arrest stress intensity factor threshold |
| $\Delta K_{eff}$ | effective stress intensity factor range |
| $\delta$ | fretting displacement |
| $\delta^*$ | fretting displacement amplitude |
| $\varepsilon^p_{11}$ | plastic strain |
| $\gamma_e$ | kinematic hardening coefficient |
| $\nu$ | Poisson coefficient |
| $\Theta_i$ | angle $i$ with the normal plane of the surface |
| $\sigma_u$ | ultimate stress |
| $\sigma_{y0.2}$ | yield stress |
| $\sigma_d$ | fatigue limit |
| $\mu$ | coefficient of friction |
| $\mu_t$ | coefficient of friction at the sliding transition |
| $\mu_{crack}$ | coefficient of friction in the crack |

threshold ($\Delta K_{th}$), and the crack will prevent an infinite endurance response being induced (see B in Fig. 1). In contrast, if the combined fretting fatigue stress induces SIF evolution outside the material boundary, the crack will propagate until failure (see D in Fig. 1). This crack arrest description of fretting–fatigue endurance was introduced by Lindley [2] and successively extended by Araújo and Nowell [3]. To satisfy the paradox that initial fretting cracks may propagate with SIF values lower than the nominal long crack threshold ($\Delta K_0$), the authors considered a short crack correction, assuming the